Theor Chem Acc (2007) 117:555–564
DOI 10.1007/s00214-006-0188-z

REGULAR ARTICLE

Accurate and local formulation for thermodynamic properties directly from integral equation method

Shiqi Zhou

Received: 1 June 2006 / Accepted: 2 November 2006 / Published online: 10 January 2007

Abstract A local formulation for determination of excess chemical potential is derived out by applying an assumption of linear dependence of correlation function and bridge function on the charging parameter to the Kirkwood charging formula and scaling the bridge function, the scaling parameter is specified by a Gibbs–Duhem relation. The local formulation for the excess chemical potential only requires the correlation function and bridge function of the investigated state as input and is therefore free of an unwieldy thermodynamic integration. A comprehensive comparison between the presently calculated thermodynamic quantities for a Lennard–Jones (LJ) fluid including two key quantities, i.e. the excess chemical potential and excess entropy, corresponding simulation data available in literature, and corresponding calculated results by several other global and local formulations, indicates that the present formulation is the only one capable of predicting locally and excellently all of the thermodynamic properties of the LJ fluid. The GCMC simulation is carried out for a core-softened potential fluid and the LJ fluid near critical state and at subcritical state near the gas–liquid coexistence line to obtain the excess chemical potential which is also in excellent agreement with the theoretical prediction from the present formalism; this indicates that the present formalism is of general interest in fluid statistical mechanics and applicable to parameter space covering over the entire phase diagram.

S. Zhou (✉)
Institute of Modern Statistical Mechanics,
Hunan University of Technology, Wenhua Road,
Zhuzhou city, 412008, People's Republic of China
e-mail: chixiayzsq@yahoo.com

1 Introduction

Integral equation theory (IET) in classical statistical mechanics is a powerful theoretical tool for calculation of correlation functions of fluid systems [1–6]. Since the introduction of self-consistent bridge function approximation such as the well-known RY approximation due to Rogers and Young [7] in 1984, accuracy of IET has arrived at such a level that a radial distribution function (RDF) denoted by $g(r)$ predicted by the IET can be equivalent with the simulation results within numerical accuracy of the latter. In principle, thermodynamic properties also can be predicted by the IET, but an unwieldy thermodynamic integration has to be incurred. Especially, when one considers the subcritical temperature case in which the isothermal thermodynamic integration path would cross an instability region of the phase diagram, one will have to resort to a combination of both the compressibility route and the energy route to reach points of the liquid region [8], this only increases the calculational task and difficulty for coding. Therefore, it is very desirable to calculate the thermodynamic properties avoiding the thermodynamic integration. Among all the thermodynamic properties, calculation of excess chemical potential $\beta\mu^{\mathrm{ex}}$ is of paramount importance. Upon acquirement of the $\beta\mu^{\mathrm{ex}}$, all of other thermodynamic properties can be easily obtained locally. Here, the word "local" means that one can calculate the desirable quantities with only the correlation function of the considered state as input, and avoid the unwieldy thermodynamic integration.

The present report is organized as follows. In Sect. 2, the present local formulation for calculation of the $\beta\mu^{\mathrm{ex}}$ is derived out theoretically, then the formulation is employed to calculate locally the $\beta\mu^{\mathrm{ex}}$ and excess

entropy S^{ex} of a Lennard–Jones (LJ) fluid in combination with the framework of a modified hypernetted chain (MHNC) approximation. To evaluate the validity of the present formulation, the present calculational results are compared with those based on several previous formulations and computer simulation. In the same Sect. 2, we also carry out Grand Canonical Ensemble Monte Carlo (GCEMC) simulations for the LJ fluid and a core-softened potenial fluid at constant chemical potential μ, volume V, and temperature T, and provide new simulation data for the $\beta\mu^{ex}$ in the "dangerous" regions of the bulk phase diagram to give a stringent test of the present formulation. To show the practical effectiveness, the present local formulation is employed to construct the liquid–gas phase diagram of the LJ fluid and compared with the computer simulation results available in literature. Finally, we conclude the present findings in Sect. 3.

2 Local formulation for the excess chemical potential and test

The fluid IET is based on an exact Ornstein–Zernike (OZ) integral equation (IE) [1–6]:

$$h(r) - C_0^{(2)}(r) = \rho \int d\mathbf{r}_1 h(\mathbf{r}_1) C_0^{(2)}(|\mathbf{r} - \mathbf{r}_1|), \tag{1}$$

to determine the total correlation function $h(r) = [g(r) - 1]$, the second-order direct correlation function (DCF) $C_0^{(2)}(r)$, and the indirect correlation function $\gamma(r) = [h(r) - C_0^{(2)}(r)]$, the OZ IE has to be solved together with a closure relation written in a formally exact expression:

$$g(r) = \exp\{-\beta u(r) + \gamma + B(r)\} \tag{2}$$

where $\beta = \frac{1}{k_B T}, k_B$ being Boltzmann constant, and T being absolute temperature, ρ being particle number density and $u(r)$ is the interparticle potential function. It should be pointed out that only the separation argument r appears in the above quantities, but these quantities also depend on other arguments which we ignore for convenience and simplicity. However, some of these arguments will be written out explicitly when needed.

Equation (2) depends on a so-called bridge function $B(r)$ which is a sum of "bridge" or "elementary" graphs in the diagrammatic analysis of the two-point functions. Although there exists a formal relationship between $B(r)$ and $g(r)$, it involves an infinite sum of highly connected diagrams [1–6] which render its utilization in practical calculation impossible. Therefore, the bridge function has to be approximated to find a concrete solution of the OZ IE.

The Gibbs–Duhem (GD) relation that links the $\beta\mu^{ex}$ to the pressure P via the fluctuation route, provides the following expression for the $\beta\mu^{ex}$:

$$\beta\mu^{ex} = -4\pi \int_0^\rho d\rho' \int dr r^2 C_0^{(2)}(r;\rho'). \tag{3}$$

Obviously, the GD relation is concerned with a thermodynamic integration along an isothermal path.

In addition, there also exist two other independent routes from correlation function knowledge to the $\beta\mu^{ex}$. Namely, the classical formula of Kirkwood [9] on the one hand, and that based on the activity [10] on the other hand. In order to implement a numerical evaluation, the former demands, for aim of integration, numerous calculations of the pair correlation functions with different value of the charging parameter, while the latter is more straightforward, but its local formulation is an approximation in terms of the bridge function. Nevertheless, Kjellander and Sarman [11], and later Lee [12] derived out a direct expression within Kirkwood's formula which is also convenient and local.

The classical formula of Kirkwood is given by

$$\beta\mu^{ex} = \rho \int_0^1 d\lambda \int d\mathbf{r} \frac{\partial \beta u(r,\lambda)}{\partial \lambda} g(r,\lambda), \tag{4}$$

where λ is the charging (coupling) parameter. An exact expression equivalent to Eq. (4) was found by Kjellander and Sarman [11], and Lee [12],

$$\beta\mu^{ex} = \rho \int_0^\infty \left(\gamma(r) - h(r) + B(r) + \frac{1}{2}h(r)\gamma(r) + \int_0^1 d\lambda h(r,\lambda)\frac{\partial B(r,\lambda)}{\partial \lambda}\right) 4\pi r^2 dr. \tag{5}$$

If one assumes a linear dependence of the correlation function $h(r,\lambda)$ on λ, namely

$$h(r,\lambda) = \lambda h(r), \tag{6}$$

one obtains

$$\beta\mu^{ex} = \rho \int_0^\infty \left(\gamma(r) - h(r) + B(r) + \frac{1}{2}h(r)\gamma(r) + h(r)\int_0^1 d\lambda \lambda \frac{\partial B(r,\lambda)}{\partial \lambda}\right) 4\pi r^2 dr, \tag{7}$$

if one further assumes an unique functionality of the bridge function, i.e. $B(r) = B(\gamma^*(r))$, a path dependence

may be introduced and Eq. (7) can be rewritten as

$$\beta\mu^{\mathrm{ex}}=\rho\int_0^{\infty}\left(\gamma(r)-h(r)+B(r)+\frac{1}{2}h(r)\gamma(r)\ +h(r)B(r)\right.$$
$$\left.-\frac{h(r)}{\gamma^*(r)}\int_{-\beta u_2(r)}^{\gamma^*(r)}B(\gamma')\mathrm{d}\gamma'\right)4\pi r^2\mathrm{d}r, \qquad (8)$$

where $\gamma^*(r)$ is a renormalized $\gamma(r)$ [12], and $-\beta u_2(r)$ is the renormalized potential. Equation (8) is exactly the formula used by Lee [12].

Kiselyov and Martynov [13] proposed another local formulation for the $\beta\mu^{\mathrm{ex}}$,

$$\beta\mu^{\mathrm{ex}}=\rho\int_0^{\infty}\left(\gamma(r)-h(r)+B(r)\right.$$
$$\left.+\frac{1}{2}h(r)\Big(\gamma(r)+B(r)+B^1(r)\Big)\right)4\pi r^2\mathrm{d}r. \qquad (9)$$

It was shown that the $B^1(r)$ is an infinite series of irreducible diagrams, but unfortunately cannot be summed up exactly. Little is known about it, excepted that at low densities $B^1(r)=\frac{1}{3}B(r)$ [14], at high densities, the relation between $B^1(r)$ and $B(r)$ remains still unknown. In Refs. [14,15], the equality $B^1(r)=\frac{1}{3}B(r)$ is used in Eq. (9) to calculate the μ^{ex} of the LJ fluid, i.e.

$$\beta\mu^{\mathrm{ex}}=\rho\int_0^{\infty}\left(\gamma(r)-h(r)+B(r)\right.$$
$$\left.+\frac{1}{2}h(r)\Big(\gamma(r)+\frac{4}{3}B(r)\Big)\right)4\pi r^2\mathrm{d}r. \qquad (9')$$

It should be mentioned that the expression Eq. (9′) is more convenient than the former one given by Eq. (8) since it does not require any analytic expression of $B(r)$ as a function of $\gamma(r)$ or $\gamma^*(r)$. It is interesting to point out that these two expressions are based on two independent routes. The former is derived from the Kirkwood's formula in which the charging parameter accounts for an insertion of a particle in the fluid, the latter is based on the activity in which $\beta\mu^{\mathrm{ex}}$ is expressed in terms of the one-particle DCF.

Besides the global formulation Eq. (3), two local formulations Eqs. (8) and (9′), there also exists a variant [16] of the Eqs. (9, 9′):

$$\beta\mu^{\mathrm{ex}}=\rho\int_0^{\infty}\Big(\gamma(r)-h(r)+B(r)+\frac{1}{2}h(r)$$
$$\times\big(\gamma(r)+B(r)+\alpha\big(\rho^*,T^*\big)B(r)\big)\Big)4\pi r^2\mathrm{d}r, \qquad (9'')$$

where $\alpha(\rho^*,T^*)$ in Eq. (9″) is determined by a sum rule Eq. (12) as will be detailed later.

Now we will derive out a new local formulation starting from Eq. (5). We assume that both the correlation function $h(r,\lambda)$ and bridge function $B(r,\lambda)$ depend on linearly λ, namely, the equality $B(r,\lambda)=\lambda B(r)$ and Eq. (6) hold; then one obtains

$$\beta\mu^{\mathrm{ex}}=\rho\int_0^{\infty}\Big(\gamma(r)-h(r)+B(r)$$
$$+\frac{1}{2}h(r)(\gamma(r)+B(r))\Big)4\pi r^2\mathrm{d}r. \qquad (10)$$

Considering that the $\beta\mu^{\mathrm{ex}}$ depends explicitly on the bridge function $B(r)$ and it has been shown that its calculation is mainly affected by the contribution of $B(r)$ inside the core (98% in the case of hard sphere fluid [12]). That is the reason why a highly reliable bridge function is necessary to calculate accurately the $\beta\mu^{\mathrm{ex}}$. On the other hand, for case of fluid whose interparticle potential includes a strongly repulsive core, an approximation for the bridge function, even if it can predict accurately the RDF, maybe quantitatively very inaccurate, or even qualitatively incorrect inside the core. Since the RDF does not depend on the bridge function inside the core, only depends on the bridge function outside the core. Therefore, one cannot judge the performance of a bridge function approximation only by the predicted RDF. To compensate for the inaccuracy of the bridge function approximation inside the core, we suggest scaling the bridge function in Eq. (10), i.e. we use following equality instead of Eq. (10)

$$\beta\mu^{\mathrm{ex}}=\rho\int_0^{\infty}\Big(\gamma(r)-h(r)+\alpha\big(\rho^*,T^*\big)B(r)$$
$$+\frac{1}{2}h(r)\big(\gamma(r)+\alpha\big(\rho^*,T^*\big)B(r)\big)\Big)4\pi r^2\mathrm{d}r \qquad (11)$$

where $\rho^*=\rho\sigma^3, T^*=\frac{k_{\mathrm{B}}T}{\varepsilon}$ are, respectively, reduced density and reduced temperature of the bulk fluid, ε being energy parameter and σ being size parameter of the interaction potential as will be pointed out later. Upon acquirement of the correlation functions, the scaling parameter $\alpha(\rho^*,T^*)$ is determined by the sum rule:

$$\beta\frac{\partial\mu^{\mathrm{ex}}}{\partial\rho}\bigg|_{\rho^*,T^*} = -4\pi\int \mathrm{d}r r^2 C_0^{(2)}(r;\rho). \tag{12}$$

Equation (12) is the differential form of the GD relation, Eq. (3).

The derivative associated with Eq. (12) is calculated by finite-difference method and ignoring the density dependence of the scaling parameter $\alpha(\rho^*, T^*)$,

$$\beta\frac{\partial\mu^{\mathrm{ex}}}{\partial\rho}\bigg|_{\rho^*,T^*} = \frac{\beta\mu^{\mathrm{ex}}(\rho^*+\Delta\rho^*,T^*,\alpha(\rho^*,T^*)) - \beta\mu^{\mathrm{ex}}(\rho^*,T^*,\alpha(\rho^*,T^*))}{\Delta\rho}, \tag{13}$$

where $\Delta\rho^*$ is a small density increment (usually 10^{-4} in ρ^* units).

To test the validity of the present local formulation, we will employ the Eq. (11) to calculate the thermodynamic properties of the LJ fluid which is extensively investigated by theories and simulation, this enables one to give a comprehensive comparison between the present Eq. (11), other published local formulations, Eqs. (8, 9′, 9″), and a global formulation, Eq. (3). To initiate the numerical implementation of Eq. (11), one has to import correlation function and bridge function of the LJ fluid; we will obtain these quantities in the framework of the MHNC approximation [17,18] for the OZ IE. In the MHNC approximation [17,18], $B(r) = B_{\mathrm{hs}}(r; d_{\mathrm{e}})$, here, $B_{\mathrm{hs}}(r;\sigma_{\mathrm{HS}})$ is the hard sphere bridge function, d_{e} and σ_{HS} are, respectively, an effective hard sphere diameter and the hard sphere diameter. In the present investigation, we employ the following approximate hard sphere bridge function given by

$$\begin{aligned} B_{\mathrm{hs}}(r;\sigma_{\mathrm{HS}}) &= \ln(y(r)) + 1 + C_{\mathrm{hs}}(r) \quad r < \sigma_{\mathrm{HS}} \\ &\quad \ln(g(r)) + C_{\mathrm{hs}}(r) + 1 - g(r) \quad r > \sigma_{\mathrm{HS}}, \end{aligned} \tag{14}$$

where, $\ln(y(r))$—logarithm of the hard sphere cavity correlation function, is given by a simulation data-fitting formula due to Ballance and Speedy [19]; $C_{\mathrm{hs}}(r)$, the second order DCF of hard sphere fluid, is given by simulation data-fitting formula due to Groot, van der Eerden, and Faber [20]; Finally, $g(r)$ is given by simulation data-fitting formula due to Verlet and Weis [21]. Therefore, we call the Eq. (14) GvEF–BS–VW bridge function.

The effective hard sphere diameter d_{e} associated with the MHNC procedure is specified by enforcing a local consistency condition, i.e. the reduced isothermal compressibility from the virial route and the fluctuation route should be equal. The virial reduced isothermal compressibility $\frac{\chi_0}{\chi_T^{\mathrm{v}}}$ is calculated by the finite-difference method, usually one assumes an equal value of the d_{e} at the density ρ^* and $\rho^* + d\rho^*$, where $d\rho^*$ is a conveniently small density increment (typically 10^{-4} in ρ^* units). Thus one obtains

$$\frac{\chi_0}{\chi_T^{\mathrm{v}}} = \beta\frac{\partial P^{\mathrm{v}}}{\partial\rho} = \frac{\beta P^{\mathrm{v}}(\rho^*+d\rho^*,T^*,d_{\mathrm{e}}) - \beta P^{\mathrm{v}}(\rho^*,T^*,d_{\mathrm{e}})}{d\rho}, \tag{15}$$

the virial pressure P^{v} is calculated from the virial route

$$\frac{\beta P^{\mathrm{v}}}{\rho} = 1 - \frac{\beta\rho}{6}\int_0^{\infty} \mathrm{d}r 4\pi r^3 \frac{\mathrm{d}u(r)}{\mathrm{d}r} g(r). \tag{16}$$

The reduced isothermal compressibility $\frac{\chi_0}{\chi_T^{\mathrm{c}}}$ throughout the fluctuation route reads

$$\frac{\chi_0}{\chi_T^{\mathrm{c}}} = \beta\frac{\partial P^{\mathrm{c}}}{\partial\rho} = 1 - \rho\int \mathbf{d}\mathbf{r} C_0^{(2)}(r;\rho), \tag{17}$$

where $\chi_0 = (\rho k_{\mathrm{B}} T)^{-1}$ is the ideal gas compressibility. Equality between $\beta\frac{\partial P^{\mathrm{v}}}{\partial\rho_b}$ and $\beta\frac{\partial P^{\mathrm{c}}}{\partial\rho}$ provides an equation for determination of the d_{e}.

The LJ potential is given by

$$u(r) = 4\varepsilon\left[\left(\frac{r}{\sigma}\right)^{-12} - \left(\frac{r}{\sigma}\right)^{-6}\right]. \tag{18}$$

Upon acquirement of the correlation functions, one can easily obtain the $\beta\mu^{\mathrm{ex}}$ by Eq. (11), virial pressure P^v by Eq. (16), excess internal energy per particle $\frac{\beta U^{\mathrm{ex}}}{N}$ by Eq. (19), and excess entropy S^{ex} by Eq. (20),

$$\frac{\beta U^{\mathrm{ex}}}{N} = 2\pi\rho\int \beta u(r) g(r) r^2 \mathrm{d}r \tag{19}$$

$$S^{\mathrm{ex}} = \frac{\beta P}{\rho} - 1 + \frac{\beta U^{\mathrm{ex}}}{N} - \beta\mu^{\mathrm{ex}} \tag{20}$$

The present calculational results together with those theoretical results from Ref. [15] based on Eqs. (3) and (9′), respectively, are presented in Table 1 for two subcritical temperature cases. It can be easily concluded that for the prediction of the S^{ex}, the local formulation —Eq. (8)—almost fail completely (see Table 1 of Ref. [15]), the Eqs. (3) and (9′) improve on the Eq. (8) greatly, but are still very unsatisfactory when the density becomes higher. For example, for case of $\rho^* = 0.87$ and $T^* = 0.75$, the percent relative errors (PRE) for the S^{ex} of Eq. (3), (8), and (9′) are, respectively, 11.257, 81.334, and 15.674, while the PRE of the present Eq. (11) is only 3.178. For case of Table 1, both the present OZ ITE based on the MHNC–GvEF–BS–VW bridge function and that based on the VM bridge function [15] perform very well for the excess internal energy. But when the compressibility factor $Z = \frac{\beta P}{\rho}$ is very low, the two PREs for the Z is significant. However, the absolute error is not significant. Another reason explaining the significant PREs of the present OZ IET and that in Ref. [15]

Table 1 Excess internal energy $U^{ex}/U^{ex}N\varepsilon\, N\varepsilon$, compressibility factor $Z = \beta P^{v}/\beta P^{v}\rho\,\rho$, and excess entropy S^{ex} of the Lennard–Jones (LJ) fluid calculated with the present MHNC–GvEF–BS–VW bridge function—Eq. (11)

T^*	ρ^*	$U^{ex}/N\varepsilon$	$U^{exJC}/N\varepsilon$	$U^{ex}_{MD}/N\varepsilon$	Z	Z^{JC}	Z_{MD}	S^{ex}	$S^{ex,JC,KM}$	$S^{ex,JC,GD}$	$S^{ex,HV}$
1.15	0.5	−3.4788	−3.4519	−3.499[a]	−0.07723	−0.2046		−1.4726	−1.4778	−1.4778	−1.457
1.15	0.6	−4.1121	−4.1093	−4.130[a]	0.05099	0.0274		−1.8217	−1.8530	−1.9213	−1.815
1.15	0.65	−4.4477	−4.4461	−4.458[a]	0.2734	0.2619		−2.0356	−2.0929	−2.1955	−2.037
1.15	0.75	−5.1009	−5.1001	−5.108[b]	1.1666	1.1721	1.161[b]	−2.5273	−2.6565	−2.7759	−2.556
1.15	0.85	−5.6600	−5.6666	−5.665[b]	2.8946	2.8675	2.865[b]	−3.1489	−3.3462	−3.3920	−3.150
1.15	0.92	−5.9407	−5.9678	−5.953[b]	4.7994	4.6702	4.719[b]	−3.6323	−3.9193	−3.8318	−3.625
1.15	0.93	−5.9752	−6.0023	−5.986[b]	5.1050	4.9768	5.022[b]	−3.7495	−4.0081	−3.8943	−3.671
1.15	0.94	−6.0058	−6.0342	−6.013[b]	5.4307	5.2967	5.364[b]	−3.8692	−4.0988	−3.9564	−3.739
1.15	0.95	−6.0324	−6.0637	−6.039[b]	5.7776	5.6303	5.711[b]	−3.9640	−4.1912	−4.0182	−3.810
1.15	0.96	−6.0556	−6.0904	−6.063[b]	6.1417	5.9779	6.069[b]	−4.0733	−4.2854	−4.0795	−3.882
1.15	0.97	−6.0757	−6.1144	−6.082[b]	6.5525	6.3400	6.450[b]	−4.1319	−4.3817	−4.1404	−3.953
0.75	0.7	−5.0540	−5.0457	−5.076[a]	−1.6398	−1.6179	−0.812[a]	−2.6003	−2.7760	−2.7760	−2.595
0.75	0.8	−5.7618	−5.7530	−5.772[a]	−0.4079	−0.3555	−0.294[a]	−3.2234	−3.5719	−3.5430	−3.226
0.75	0.84	−6.0209	−6.0152	−6.024[b]	0.4749	0.4973	0.441[b]	−3.5435	−3.9389	−3.8465	−3.441
0.75	0.85	−6.0821	−6.0777	−6.084[b]	0.7367	0.7466	0.692[b]	−3.6311	−4.0351	−3.9217	−3.516
0.75	0.86	−6.1419	−6.1389	−6.134[b]	1.0129	1.0112	0.952[b]	−3.7352	−4.1330	−3.9967	−3.581
0.75	0.87	−6.1976	−6.1984	−6.192[b]	1.3288	1.2918	1.244[b]	−3.7753	−4.2325	−4.0709	−3.659

The superscript JC denotes theoretical results from Ref. [15]; KM and GD have the same meaning as in Ref. [15]; absence of the superscript and subscript denotes the present results; superscript HV denotes simulation data from Hansen and Verlet [25]
[a]Subscript MD denotes molecular dynamics simulation data from Ref. [23]
[b]Subscript MD denotes molecular dynamics simulation data from Ref. [24]

is due to inaccuracy of the simulational Z. Taking the case of $\rho^* = 0.7$ and $T^* = 0.75$ as an example, the present Eq. (11) predicts the S^{ex} with a PRE of only 0.2042, the excess internal energy with a PRE of 0.4334; The present Eq. (11) predicts $\beta\mu^{ex} = -6.7768$, the accurate simulation-fitting EOS in Ref. [22] predicts $\beta\mu^{ex} = -6.7422$; therefore, the PRE for the excess chemical potential is also only 0.5132. According to Eq. (20), the Z should be −1.6386, in very good agreement with the present virial compressibility factor: −1.6383. Therefore, one can suspect that there exist large error associated with the molecular dynamic simulation data [23,24] for the Z when the absolute value of the Z is low.

In Table 2, the present predictions for the thermodynamic properties of LJ fluid are presented together with the corresponding simulation data [22] and that from an OZ IET in Ref. [26], where the calculation of the $\beta\mu^{ex}$ is based on Eq. (8). It can be seen out clearly that for predictions of the $\beta\mu^{ex}$, the maximum PRE in Ref. [26] is 12 for case of a combination of $\rho^* = 0.95$ and $T^* = 1.35$, the maximum PRE of the OZ IET in Ref. [14] is 16.9154 (calculated from the data collected in Table 1 of Ref. [26]) for case of a combination of $\rho^* = 0.4$ and $T^* = 2.74$, while for the present MHNC–GvEF–BS–VW bridge function and Eq. (11), the maximum PRE is only 2.77 for case of a combination of $\rho^* = 0.95$ and $T^* = 1.35$. It should be noted that in Ref. [14] the calculation of the $\beta\mu^{ex}$ is based on Eq. (9′). For other thermodynamic properties such as the $\frac{\beta U^{ex}}{N}$ and compressibility factor Z, the present MHNC-GvEF-BS-VW bridge function also performs better than that in Refs. [14,26], but the difference of the performance is not so significant as displayed in the present Table 2 for the prediction of the $\beta\mu^{ex}$. Therefore, one can confidently conclude that the present Eq. (11) is largely superior to Eqs. (8) and (9′).

One may refute that the excellent performance of the present Eq. (11) is mainly due to the scaling parameter $\alpha(\rho^*, T^*)$. To indicate that the excellent performance of Eq. (11) is mainly due to a correct inherent structure of Eq. (11), in Table 3 we compare, not only the scaling parameter $\alpha(\rho^*, T^*)$, but also the present predictions for the $\beta\mu^{ex}$ and S^{ex} of the LJ fluid with the corresponding prediction from Ref. [16], where the Eq. (9″) is employed for calculation of the $\beta\mu^{ex}$ and the required correlation functions are also from an OZ IET but based on a new bridge function approximation [16]. From Table 3, one can estimate that the maximum PRE for the $\beta\mu^{ex}$ is 12.4528 for Eq. (9″), but only 2.22 for the present Eq. (11), the maximum PRE for the S^{ex} is 6.3927 for Eq. (9″), but only 1.7146 for the present Eq. (11). Considering that both the present Eq. (11) and Eq. (9″) are concerned with the scaling parameter, and the scaling parameter is specified by the same sum rule, the significantly higher accuracy of the present Eq. (11) compared with the Eq. (9″) confidently proves that the Eq. (11) is surely structured far more soundly than Eq. (9″). It should be pointed out that although the present MHNC

Table 2 Thermodynamic properties of the LJ fluid at several supercritical temperatures

$s\rho^*$	$-\beta U^{ex}$	$-\beta U^{ex,bb}$	$-\beta U^{ex,s}$	Z	Z^{bb}	Z^{s}	$\beta\mu^{ex}$	$\beta\mu^{ex,bb}$	$\beta\mu^{ex,s}$
$T^* = 5$									
0.1	0.1022	0.102	0.101	1.0662	1.066	1.069	0.1246	0.125	0.129
0.3	0.2984	0.298	0.299	1.3243	1.318	1.327	0.5541	0.553	0.562
0.5	0.4706	0.471	0.475	1.8711	1.863	1.860	1.3769	1.370	1.371
0.7	0.5774	0.580	0.581	2.9570	2.940	2.932	2.8976	2.809	2.883
0.9	0.5370	0.540	0.538	4.9730	4.950	4.930	5.5967	5.268	5.582
1.1	0.2214	0.226	0.225	8.4763	8.446	8.418	10.2166	9.366	10.167
1.2	−0.090233	−0.091	−0.077	10.9963	10.990	10.993	13.5545	12.350	13.432
$T^* = 2.74$									
0.1	0.2227	0.222	0.222	0.9738	0.974	0.977	−0.06128	−0.061	−0.056
0.2	0.4396	0.439	0.439	0.9882	0.990	0.993	−0.06315	−0.058	−0.053
0.3	0.6523	0.652	0.653	1.0574	1.050	1.060	0.01281	0.018	0.022
0.4	0.8620	0.862	0.862	1.2060	1.197	1.204	0.1973	0.210	0.201
0.5	1.0670	1.067	1.066	1.4726	1.456	1.469	0.5372	0.550	0.536
0.6	1.2597	1.261	1.257	1.9199	1.893	1.914	1.1001	1.091	1.103
0.7	1.4265	1.426	1.421	2.6207	2.601	2.616	1.9810	1.925	1.996
0.8	1.5461	1.547	1.539	3.6791	3.656	3.665	3.3052	3.113	3.324
0.9	1.5913	1.593	1.587	5.2163	5.184	5.174	5.2207	4.789	5.229
1.0	1.5317	1.531	1.532	7.3587	7.339	7.294	7.9364	7.145	7.892
$T^* = 1.35$									
0.1	0.5793	0.580	0.575	0.7180	0.718	0.722	−0.5773	−0.575	−0.571
0.2	1.1337	1.131	1.121	0.4932	0.495	0.507	−1.0680	−1.056	−1.049
0.35	1.8363	1.822	1.839	0.3147	0.298	0.327	−1.5713	−1.556	−1.557
0.4	2.0482	2.036	2.061	0.2897	0.261	0.303	−1.6842	−1.668	−1.674
0.5	2.4957	2.487	2.510	0.3148	0.266	0.329	−1.8087	−1.765	−1.802
0.6	2.9742	2.967	2.984	0.5574	0.507	0.566	−1.6624	−1.583	−1.671
0.7	3.4504	3.440	3.461	1.2081	1.194	1.202	−1.0683	−0.944	−1.060
0.8	3.8749	3.859	3.886	2.4672	2.487	2.438	0.2681	0.283	0.274
0.9	4.1873	4.165	4.199	4.5880	4.639	4.516	2.6915	2.347	2.633
0.95	4.2804	4.253	4.290	6.0571	6.130	5.981	4.4448	3.808	4.325

The superscript bb denotes results from Ref. [26], superscript s denotes simulation data from Ref. [22], while absence of the superscript denotes the present results calculated with the present MHNC–GvEF–BS–VW bridge function—Eq. (11)

bridge function and the new bridge function in Ref. [16] are not the same, as pointed out in Ref. [16], the latter has been proved to be accurate. Therefore, such comparison should be meaningful, not too misleading.

To further test the power of the present Eq. (11), we carried out Grand Canonical Ensemble Monte Carlo (GCEMC) simulations [27] at constant chemical potential μ, volume V, and temperature T, and supply new simulation data for the $\beta\mu^{ex}$ of the LJ fluid, the bulk state is near the critical point for supercritical state, or is situated near the gas–liquid coexistence line for subcritical state, simulational data for these "dangerous" regions constitute a stringent standard for check of the Eq. (11). The calculational results from the present Eq. (11) are presented in Tables 4 and 5 together with the presently new simulational data, one can see clearly out that the same excellent accuracy as displayed in Tables 1, 2, and 3 still keeps on for these "dangerous" regions'.

To indicate the applicability of the present Eq. (11) to other interaction potential fluids as well as the extensively studied LJ fluid, we also carried out the GCEMC simulations for a water-like core-softened potential fluid given by

$$\begin{aligned} u(r) =& \propto \quad r < \sigma \\ & -\delta\varepsilon \quad \sigma < r < b \\ & -\varepsilon \quad b < r < c. \end{aligned} \tag{21}$$

The core-softened potential [28], although simple, has many of the properties that characterizes water as an anomalous fluid, and gives insight into the properties of real water. For example, it reproduces anomalous thermal properties that are similar to those observed in water, and predicts liquid–liquid phase transition. Therefore, the core-softened potential has been used as a simple zeroth-order approximation of liquid water [28,29]. In fact, the simplicity of the model allows us to single out the crucial characteristic that produces all the anomalies, without the complications introduced by nonspherical interactions and cooperative hydrogen bonding in real water. Therefore, simple and accurate theoretical treatment on the core-softened potential

Table 3 Thermodynamic properties of the LJ fluid at several supercritical temperatures

ρ^*	$\alpha(\rho^*, T^*)$	$-s$	$-s^{\mathrm{bb}}$	$-s^{\mathrm{s}}$	$\beta\mu^{\mathrm{ex}}$	$\beta\mu^{\mathrm{ex,bb}}$	$\beta\mu^{\mathrm{ex,s}}$
$T^* = 5$							
0.1	0.8044	0.1606	0.161	0.161	0.1246	0.125	0.129
0.3	0.8395	0.5279	0.531	0.534	0.5541	0.551	0.562
0.5	0.8397	0.9761	0.963	0.986	1.3769	1.356	1.371
0.7	0.8502	1.5152	1.491	1.532	2.8976	2.851	2.883
0.9	0.8592	2.1635	2.050	2.190	5.5967	5.450	5.582
$T^* = 2.74$							
0.1	0.8665	0.1877	0.188	0.189	−0.06128	−0.06	−0.056
0.3	0.8621	0.6076	0.610	0.615	0.01281	0.009	0.022
0.5	0.8474	1.1304	1.142	1.133	0.5372	0.523	0.536
0.7	0.8568	1.7865	1.796	1.801	1.9810	1.971	1.996
0.9	0.8670	2.5967	2.564	2.642	5.2207	5.155	5.229
$T^* = 1.35$							
0.1	1.0834	0.2835	0.285	0.282	−0.5773	−0.576	−0.571
0.35	0.9196	0.9504	0.965	0.955	−1.5713	−1.568	−1.557
0.5	0.8637	1.3720	1.402	1.379	−1.8087	−1.818	−1.802
0.7	0.8657	2.1783	2.317	2.199	−1.0683	−0.928	−1.060
0.9	0.8703	3.3112	3.454	3.316	2.6915	2.928	2.633

The superscript bb denotes results from Ref. [16], superscript s denotes simulation data from Ref. [22], while absence of the superscript denotes the present results calculated with the present MHNC–GvEF–BS–VW bridge function—Eq. (11)

Table 4 Thermodynamic properties of the LJ fluid at near-critical temperatures

ρ^*	Z	Z^{fitting}	Z^s	$\beta\mu^{\mathrm{ex}}$	$\beta\mu^{\mathrm{ex,fitting}}$	$\beta\mu^{\mathrm{ex,s}}$
$T^* = 1.39072$						
0.10455	0.7240	0.7277	0.725666	−0.5669	−0.5600	−0.5619
0.32961	0.3743	0.3861	0.385016	−1.4225	−1.4078	−1.4102
0.49211	0.3743	0.3881	0.390341	−1.6673	−1.6605	−1.6610
0.59980	0.6496	0.6499	0.664700	−1.5000	−1.5002	−1.4888
0.70986	1.3984	1.3889	1.389270	−0.7801	−0.7682	−0.7573
0.79642	2.5006	2.4693	2.420890	0.40321	0.4131	0.4276
$T^* = 1.32250$						
0.10451	0.6940	0.6984	0.6959	−0.6273	−0.6193	−0.6215
0.37794	0.2652	0.2765	0.2685	−1.7107	−1.7015	−1.7120
0.50557	0.2710	0.2870	0.29094	−1.9103	−1.9048	−1.9029
0.70374	1.1770	1.1694	1.18745	−1.1746	−1.1648	−1.1487

The superscript "fitting" denotes results from Ref. [22], superscript s denotes the present simulation data, while absence of the superscript denotes the present results calculated with the present MHNC–GvEF–BS–VW bridge function—Eq. (11)

Table 5 Thermodynamic properties of the LJ fluid at several subcritical temperatures and near the gas–liquid coexistence line

ρ^*	Z	Z^{fitting}	Z^s	$\beta\mu^{\mathrm{ex}}$	$\beta\mu^{\mathrm{ex,fitting}}$	$\beta\mu^{\mathrm{ex,s}}$
$T^* = 1.28576$						
0.10340	0.6790	0.6840	0.681112	−0.6570	−0.6482	−0.65085
0.61270	0.4631	0.4722	0.491149	−1.9166	−1.9265	−1.91012
$T^* = 1.0496$						
0.04022	0.8069	0.8099	0.807256	−0.3878	−0.3832	−0.38661
0.68276	0.1025	0.1114	0.134102	−3.1522	−3.1417	−3.11839
$T^* = 0.8528$						
0.01635	0.8849	0.8865	0.8845	−0.2298	−0.2275	−0.22947
0.85606	1.6958	1.6464	1.67598	−2.8184	−2.8818	−2.84459

The superscript "fitting" denotes results from Ref. [22], superscript s denotes the present simulation data, while absence of the superscript denotes the present results calculated with the present MHNC–GvEF–BS–VW bridge function—Eq. (11)

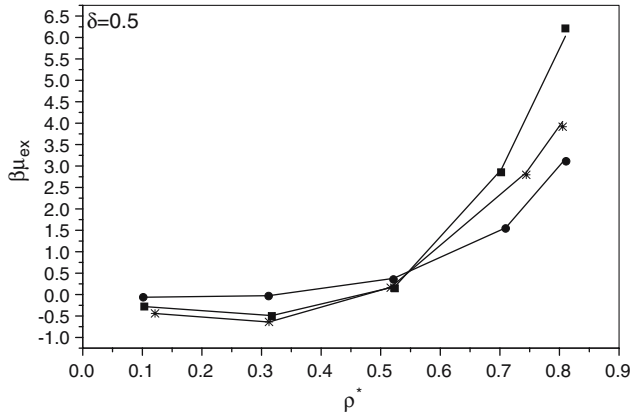

Fig. 1 The reduced excess chemical potential $\beta\mu^{\mathrm{ex}}$ versus bulk density ρ^*. *Symbols* give the present GCEMC results, the present theoretical results at the same state with the simulation are connected into a curve to guide the eye. *Circles* are for $b/\sigma = 1.1$, $c/\sigma = 1.2$, $T^* = 0.83$, *squares* are for $b/\sigma = 1.2$, $c/\sigma = 1.5$, $T^* = 1.55$, while *stars* are for $b/\sigma = 1.4$, $c/\sigma = 2$, $T^* = 3.38$

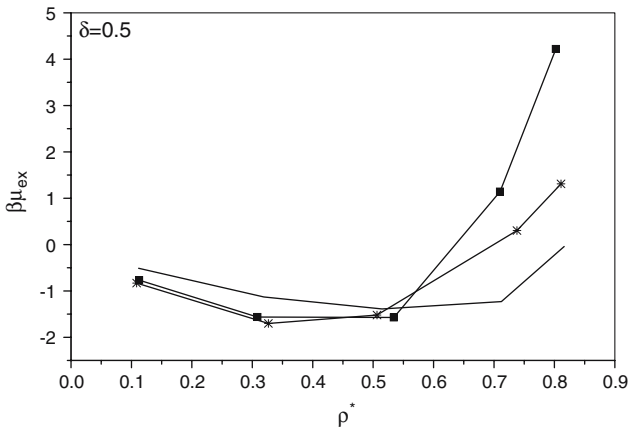

Fig. 2 The reduced excess chemical potential $\beta\mu^{\mathrm{ex}}$ versus bulk density ρ^*. *Symbols* give the present GCEMC results, the present theoretical results at the same state with the simulation are connected into a curve to guide the eye. *Circles* are for $b/\sigma = 1.1$, $c/\sigma = 1.2$, $T^* = 0.59$, *squares* are for $b/\sigma = 1.2$, $c/\sigma = 1.5$, $T^* = 1.1$, while *stars* are for $b/sigma = 1.4$, $c/\sigma = 2$, $T^* = 2.4$

fluid is very desirable, and will help greatly the investigation of water-like fluids.

In Figs. 1 and 2, the GCEMC simulation results for the $\beta\mu^{\mathrm{ex}}$ is presented together with our theoretical calculation based on the present MHNC–GvEF–BS–VW bridge function—Eq. (11). It is clearly shown that our formalism reproduces the simulation data very accurately. Considering that we are dealing with the core-softened potential of varying interaction range by choosing appropriately the potential parameters, the excellent agreement convinces one that the present Eq. (11), when in combination with the MHNC–GvEF–BS–VW bridge function procedure, is applicable to short-range potential fluid as well as the long-range potential fluid popular in simple atomic fluid. The short-range property is usually associated with an effective potential originating in a coarse-grained procedure in treating complex fluids, therefore is ubiquitous in physical systems constituted by macroparticles. The excellent performance of the present formalism opens a simple and accurate route for theoretically tackling on the complex fluids.

The idea of using a local formulation of the chemical potential is in its usefulness for the construction of the liquid–gas phase diagram. Therefore, a comparison of the latter with existing simulation data is one of the ultimate tests for the Eq. (11).

The liquid–gas coexistence occurs when at a given temperature the two phases have equal chemical potentials and pressures:

$$\mu_g(\rho_g, T) = \mu_l(\rho_l, T) \tag{22}$$

$$P_g(\rho_g, T) = P_l(\rho_l, T). \tag{23}$$

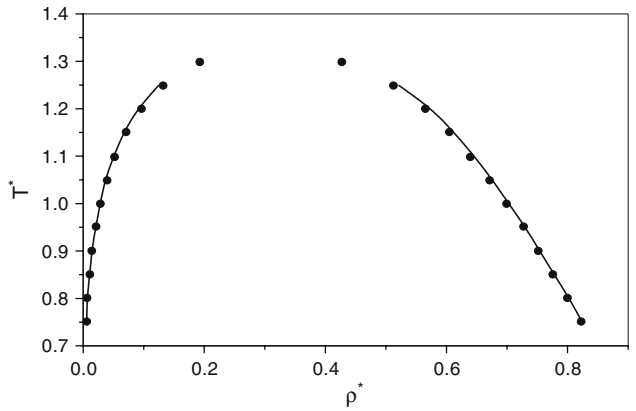

Fig. 3 The liquid–gas coexistence diagram of the LJ fluid. *Solidline* represent the results from the present formalism, while *solidcircles* represent results from the NPT simulation of Lotfi et al. (Ref. [30])

The required pressure is from the virial pressure P^v as detailed above, the chemical potentials include an ideal part μ_{id} and the excess part μ_{ex}, the μ_{ex} is calculated from the present combination of the MHNC–GvEF–BS–VW bridge function and Eq. (11), the ideal part is given by $\beta\mu_{\mathrm{id}} = \ln\left(\lambda^3\rho\right)$ with λ the thermal wavelength. The liquid–gas coexistence densities at different temperatures from the present formalism are plotted in Fig. 3 together with the same obtained by Lotfi et al. [30] from the NPT simulation. Our results show very good agreement with the simulation data, and at low temperatures it is almost identical with the simulation results. Like all other OZ IET, the present one also has convergence difficulties near the critical point; there-

fore near-critical part of the liquid–gas coexistence curve cannot be predicted by the OZ IE theory.

3 Concluding remarks

The key point of deriving the present Eq. (11) is the assumption of a linear dependence of the correlation function and bridge function on λ, i.e. $B(r,\lambda) = \lambda B(r)$ and $h(r,\lambda) = \lambda h(r)$. When $\lambda = 1$, i.e. the full potential is resumed, the assumption reduces to $B(r,1) = B(r)$ and $h(r,1) = h(r)$, which are exactly the quantities employed in the solution of the OZ IE for the full potential, therefore these two results are desirable. When $\lambda = 0$, i.e. the fluid particles are free of interaction, the assumption reduces to $B(r,0) = 0$ and $h(r,0) = 0$. For ideal gas free of interaction, it is well known that the correlation disappears; therefore the $h(r,0) = 0$ are also desirable. As for $B(r,0) = 0$, it is also desirable since weak correlation is an indication that the HNC approximation is valid, in the HNC approximation, the bridge function is zero. Since the linear assumption exactly satisfies for the two limits, one can expect that the linear assumption also should be reliable for case of $0 < \lambda < 1$.

The linear assumption also leads to undesirable property. Comparison of Eq. (10) with (9) immediately yields to the fact that $B^1(r) = 0$. As pointed out in Ref. [14], at low densities $B^1(r) = \frac{1}{3}B(r)$, on the other hand, when density tends to zero, the $B(r)$ also tends to zero. Therefore, $B^1(r)$ tends to zero when the density tends to zero. Thus, the Eq. (10) is formally exact only in the zero-density limit. Since one never knows the $B^1(r)$, one cannot evaluate quantitatively the influence of the undesirable property on the Eq. (10). As documented in Table 3, the scaling parameter $\alpha(\rho^*, T^*)$ deviates from 1, comparison of Eq. (11) with (9) yields to the fact that in Eq. (11), $B^1(r) \neq 0$. Therefore, from the view point of practical use, the Eq. (11) is not in contradiction with Eq. (9). Of course, the above qualitative analysis does not indicate that the Eq. (11) is exact, but the comparison documented in Tables 1, 2, 3, 4, and 5 and Figs. 1, 3 and 3 surely shows that the Eq. (11) is quantitatively excellent, the absence of formal contradiction between Eqs. (11) and (9) is also therefore quantitatively favourable.

What is the difference between Eqs. (11) and (9″)? From the view point of theoretical derivation, the Eq. (11) originates from importing the linear assumption into the exact Eq. (5), then scaling the bridge function in the resultant Eq. (10). While the Eq. (9″) originates simply from the exact Eq. (9) and assuming that the $B^1(r)$ can be substituted by the scaling bridge function. Although Eqs. (11) and (9″) look very similar, they are different structurally as detailed from our following explanation about the origin of the superiority of the present Eq. (11) over (9″). For interaction potentials consisting of a short-range steeply repulsive core and a tail, one only can evaluate, by the predicted RDF, the performance of any bridge function approximation, including the presently employed MHNC approximation, outside the core, i.e. how the approximation inside the core performs cannot be evaluated by the predicted RDF. However, it is exactly the inside part of the bridge function approximation that determines mainly the $\beta\mu^{\mathrm{ex}}$. Therefore, small error of the inside part of the bridge function approximation can lead to significant deviation of the resultant $\beta\mu^{\mathrm{ex}}$ from the true one. To compensate for the inaccuracy of the bridge function approximation, one has to scale the bridge function and determine the scaling parameter by an exact sum rule. However, the scaling in Eq. (9″) is only partial, there are two terms still unscaled. On the contrary, the scaling in the present Eq. (11) is complete.

To conclude, we propose a local formulation for calculation of the $\beta\mu^{\mathrm{ex}}$ only from the correlation function and bridge function of the investigated state point. To evaluate the quality of the local formulation, we apply it to calculate $\beta\mu^{\mathrm{ex}}$ and S^{ex} and other thermodynamic properties of the LJ fluid, the required correlation function is from solving numerically the OZ IE in the framework of the MHNC approximation for the bridge function. The hard sphere bridge function required as input of the MHNC approximation is of a hybrid form each part of which is based on a simulation data-fitting formula. By comparing the present predictions with corresponding molecular dynamic simulation data and Monte Carlo simulation data available in literature, and those from three previous local formulations and one global formulation, we find that the present local formulation is the most accurate among all existing local and global formulations. Even for the cases where the performance of all of other local and global formulations becomes very poor, the present Eq. (11) still performs excellently. We also carried out GCEMC simulations, a comparison between the present predictions based on the Eq. (11) and new simulation data for "dangerous" regions in the phase diagram gives positive results, and therefore one can confidently believe that the present local formulation Eq. (11) is surely a highly accurate and generally excellent approximate formula.

Acknowledgments The author is pleased to acknowledge the comments from two reviewers. This project was supported by the National Natural Science Foundation of China (Grants Nos. 20673150).

References

1. Hill TL (1960) Introduction to statistical thermodynamics, Addison Wesley, New York
2. Chandler D (1987) Introduction to modern statistical mechanics, Oxford University Press, New York
3. Sarkisov L, Tassel PRV (2005) J Chem Phys 123:164706
4. Wilson DS, Lee LL (2005) J Chem Phys 123:044512
5. Zarragoicoechea GJ, Pugnaloni LA, Lado F, Lomba E, Vericat F (2005) Phys Rev E 71:031202
6. Ricker M, Schilling R (2004) Phys Rev E 69:061105
7. Rogers FJ, Young DA (1984) Phys Rev A 30:999
8. Caccamo C, Pellicane G (2002) J Chem Phys 117:5072
9. Kirkwood JG (1935) J Chem Phys 3:300
10. Martynov GA (1992) Fundamental theory of liquids. Method of distribution functions. Adam Hilger, Bristol
11. Kjellander R, Sarman S (1989) J Chem Phys 90:2768
12. Lee LL (1992) J Chem Phys 97:8606
13. Kiselyov OE, Martynov GA (1990) J Chem Phys 93:1942
14. Sarkisov G (2001) J Chem Phys 114:9496
15. Jakse N, Charpentier I (2003) Phys Rev E 67:061203
16. Bomont J-M (2003) J Chem Phys 119:11484
17. Lado F (1973) Phys Rev A 8:2548
18. Rosenfeld Y, Ashcroft NW (1979) Phys Rev A 20:1208
19. Ballance JA, Speedy RJ (1985) Mol Phys 54:1035
20. Groot RD, van der Eerden JP, Faber NM (1987) J Chem Phys 87:2263
21. Verlet L, Weis J-J (1972) Phys Rev A 5:939
22. Johnson JK, Zollweg JA, Gubbins KE (1993) Mol Phys 78:591
23. Baranyai A, Evans DJ (1989) Phys Rev A 40:3817
24. Giaquinta PV, Giunta G, Prestipino Giarritta S (1992) Phys Rev A 45:R6966
25. Hansen JP, Verlet L (1969) Phys Rev 184:151
26. Bomont J-M, Bretonnet JL (2003) Mol Phys 101:3249
27. Frenkel D Smit B (1996) Understanding molecular simulation. Academic, Boston, MA
28. Jagla EA (1999) J Chem Phys 111:8980
29. Iwamatsu M (2003) Physica A 329:14
30. Lotfi A, Vrabec J, Fischer J (1992) Mol Phys 76:1319